Advances in Environmental Biology, 6(3): 1095-1103, 2012
ISSN 1995-0756

This is a refereed journal and all articles are professionally screened and reviewed **ORIGINAL ARTICLE**

A Novel hydrogen peroxide Biosensor Based on Modified Electrode with Hemoglobin and zinc oxide nanoparticles

[1]Masoud Negahdary, [2]Mahdi Torkamani Noughabi, [3]Esmaeil Rezaei, [4]Manouchehr Mazdapour, [5]Alireza Farasat, [6]Tahereh Arabnezhad-khanooki, [7]Batool Yousefi-telori, [8]Fazlollah Mirzaei-nasab

[1]Young Researchers Club, Marvdasht Branch, Islamic Azad University, Marvdasht, Iran
[2]Department of Basic Science, Gonabad University of Medical Sciences, Gonabad, Iran
[3]Shiraz University of medical sciences, Shiraz, Iran
[4]Department of Biology, Islamic Azad University of pharmaceutical science, Tehran, Iran
[5]Biology Group, Basic Science Faculty, IHU University, Tehran, Iran
[6]Department of Biology, Payam-e-Noor University, Isfahan, Iran
[7]Faculty of Advanced Medical Technology, Golestan University of Medical Sciences, Gorgan, Iran
[8]Department of Biology, Payam-e-Noor University, Taft, Iran

Masoud Negahdary, Mahdi Torkamani Noughabi, Esmaeil Rezaei, Manouchehr Mazdapour, Alireza Farasat, Tahereh Arabnezhad-khanooki, Batool Yousefi-telori, Fazlollah Mirzaei-nasab; A Novel hydrogen peroxide Biosensor Based on Modified Electrode with Hemoglobin and zinc oxide nanoparticles

ABSTRACT

In this study, direct electron transfer between immobilized hemoglobin (Hb) and zinc oxide nanoparticles modified carbon paste electrode was studied. Direct electrochemical response of Hb on the modified electrode can be achieved and a couple of well-defined and nearly reversible cyclic voltammetric peaks of Hb can be observed in a phosphate solution. The Hb immobilized on the Modified electrode with Zno Nps displayed a pair of redox peaks in 0.1 M pH 7.0 PBS with a formal potential of + (292 ± 2) mV (vs. SCE). Hb adsorbed on the modified electrode surface shows a good activity for the reduction of hydrogen peroxide (H_2O_2). The reduction peak currents were proportional linearly to the concentration of hydrogen peroxide. The Hb/ Zno Nps/ CPE had good repeatability and stability for the determination of H_2O_2.

Key words: *biosensor, hemoglobin, zinc oxide nanoparticles, hydrogen peroxide*

Introduction

The Nanotechnology is a technology concerning processes which are relevant to physics, chemistry and biology taking place at a length scale of one divided by 100 million of a meter[1]. Maybe a little bit more enlightening although equally naive is to say that nanotechnology is the art of producing little devices and machines, somewhat at the molecular scale [2-4]. However, the scientific definition that may be slightly involved is to say that nanotechnology is concerned with the grey area between classical mechanics and quantum mechanics [5]. Classical mechanics is the mechanics governing the motion of all the objects we can see with our naked eye. One of the more advanced areas in this field currently involves the use of metal and semiconductor nanoparticles (NPs) in biological sensing applications [6]. The many techniques of immobilization of biomolecules on the surface of magnetic nanoparticles have enabled the production of bioconjugates with magnetic properties and these substances are useful for the delivery and recovery of biomolecules in biomedical applications [7-9]. A very important property of this type of nanoparticles for electrochemical biosensors is their ability to provide a favorable microenvironment for biomolecules such as proteins to exchange electrons directly with an electrode [10-11], thus improving the sensitivity of electrochemical biosensors. In this research we used of hemoglobin as protein structure; the prosthetic group of Hb is heme, which consists of protoporphyrin IX combined with a Fe^{2+} ion. The iron atom in heme is capable of making six bonds. It makes four to the pyrrole nitrogens of the porphyrin ring and another one to one of the histidine side chain of the protein, called the proximal histidine. The iron atom makes its sixth bond to O_2. Hb can only carry O_2 when its iron is in the Fe^{2+} form. If the iron is oxidised to the Fe^{3+} form the Hb is no longer

Corresponding Author

Masoud Negahdary, Young researchers club, Marvdasht branch, Islamic Azad University, Marvdasht, Iran.
E-mail: masoudnegadary@yahoo.com, Tel: +98-919-007-2275

functional and it is then known as methemoglobin[12]. Since hemoglobin is a physiological oxygen transport protein and acts as an important protein in life, it could be utilized as an ideal model protein to explore the relative biological process and redox behavior of heme proteins or enzymes. However, studies on the structure–function relationship of hemoglobin have intrigued researchers over the past years [13-15]. It is well known that the redox centers are deeply immersed in hemoglobin, so the direct electron transfer between hemoglobin and the electrode surface is rather difficult, which could cause the low rate of electron transfer between hemoglobin and the solid electrode. Recently, some methods have been explored for facilitating the relative electron transfer of hemoglobin through combining with the mediators, promoters, and some special electrode materials [16-18]. We used of zinc oxide nanoparticles for increasing rate of direct electron transfer between hemoglobin and carbon paste electrode. Electrochemical detection is of particular significance in the development of aptasensors since it allows for high sensitivity and selectivity, simple instrumentation, as well as low endogenetic background[19]. Zinc oxide (ZnO), a versatile semiconductor material, has been attracting attention because of the commercial demand for optoelectronic devices operating at blue and ultraviolet regions [20]. ZnO is a wurtzite-type semiconductor with band gap energy of 3.37 eV and it has very large excitation binding energy (60 meV) at room temperature [21-23]. Recently, special attention has been devoted to the morphology, as ZnO can form different nanostructures [24]. In overall, Electron transfer in biological system is one of the leading areas in biochemical and biophysical research fields [25-27]. The redox mechanism of proteins and the respective metabolic process of enzymes could be revealed on the basis of the direct electron transfer of proteins or enzymes, which could play a fundamental role in the life sciences and biomedical engineering [28-30]. In this study we used of direct electron transfer for designing a novel biosensor that described in flow.

2. Experimental:

2.1. Materials:

Hemoglobin was purchased from Sigma. The phosphate buffer solution (PBS) consisted of a potassium phosphate solution (KH_2PO_4 and K_2HPO_4 from Merck; 0.1 M total phosphate) at pH 7.0. All other chemicals were of analytical grade and were used without further purification. All solutions were made up with doubly distilled water.

2.2. Apparatus:

Cyclic voltammetric experiments were performed with a model EA-201 Electro Analyzer (chemilink systems), equipped with a personal computer was used for electrochemical measurement and treating of data. A conventional three electrode cell was employed throughout the experiments, with bare or Zno nanoparticles modified carbon paste electrode (3.0 mm diameter) as a working electrode, a saturated calomel electrode (SCE) as a reference electrode and a platinum electrode as a counter electrode. The phase characterization was performed by means of X-ray diffraction (XRD) using a D/Max-RA diffractometer with CuKα radiation. Samples were measured and recorded using a TU-1901 double-beam UV–visible spectrophotometer were dispersed in toluene solution. The morphologies and particle sizes of the samples were characterized by JEM-200CX transmission electron microscopy (TEM) working at 200 kV and Scanning electron microscopy (SEM) images were obtained with a ZIESS EM 902A scanning electron microscope.

2.3. Procedure:

2.3.1 Synthesis of ZnO NPs:

To prepare of ZnO NPs, in a typical experiment, a 0.45 M aqueous solution of zinc nitrate ($Zn(NO_3)_2.4H_2O$) and 0.9 M aqueous solution of sodium hydroxide (NaOH) were prepared in distilled water. Then, the beaker containing NaOH solution was heated at the temperature of about 55 ºC. The $Zn(NO_3)_2$ solution was added drop wise (slowly for 1h) to the above heated solution under high speed stirring. The beaker was sealed at this condition for 2 h. The precipitated ZnO NPs was cleaned with deionized water and ethanol then dried in air atmosphere at about 60 ºC.

2.3.2. Preparation of Carbon paste electrode:

The carbon powder (particle size 50 mm, density 20-30g/100mL) was mixed with the binder, silicone oil, in an agate mortar and homogenized using the pestle. The electrode consisted of a Teflon well, mounted at the end of a Teflon tube. The prepared paste was filled into the Teflon well. A copper wire fixed to a graphite rod and inserted into the Teflon tube served to establish electrical contact with the external circuit. The electrode surface of the working electrode was renewed mechanically by smoothing some paste off and then polishing on a piece of transparent paper before conducting each of the experiments. The experiments were performed in unstirred solutions.

2.3.3. Preparation of Zno nanoparticles modified carbon paste electrode:

The Zno nanoparticles modified carbon paste electrode was prepared by hand mixing of carbon powder, binder and 10 mg Zno nanoparticle with silicon oil in an agate mortar to produce a homogenous carbon paste. Other steps of produced modified carbon paste electrode were similar to preparation of bare carbon paste electrode. A conventional three electrode cell was employed throughout the experiments, with bare or ZnO nanoparticles modified carbon paste electrode (3.0 mm diameter) as a working electrode, a saturated calomel electrode (SCE) as a reference electrode and a platinum electrode as a counter electrode.

3. Results:

3.1. Electron microscopic investigation of Zno nanoparticles:

Morphology of the sample was investigated using SEM and TEM. Parts (A) and (B) of Figure 1 show the typical SEM and TEM images of the sample respectively. The SEM image was captured in 10-nanometer size of Zno nanoparticles and the TEM image was captured in 20-nanometer size of Zno nanoparticles.

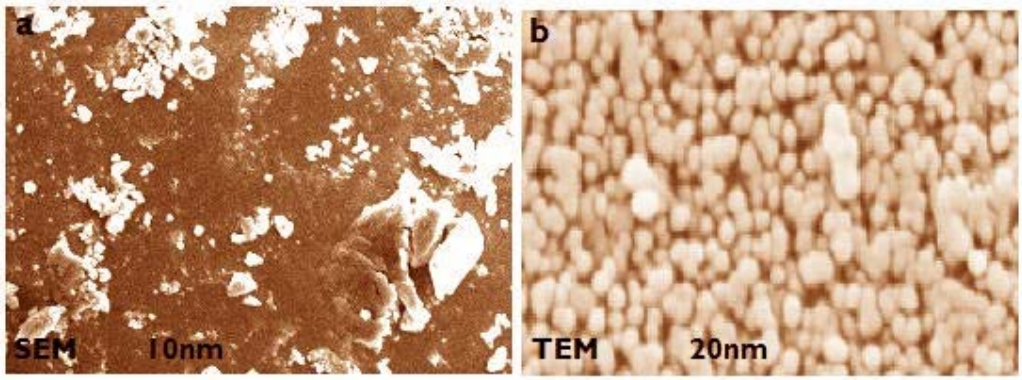

Fig. 1: (a) SEM image and (b) TEM image, of ZnO NPs.

3.2. X-Ray diffraction of Zno nanoparticles:

The x-ray diffraction data were recorded by using Cu Kα radiation (1.5406 A^o). The intensity data were collected over a 2θ range of 20-80^o. The average grain size of the samples was estimated with the help of Scherrer equation using the diffraction intensity of (101) peak. x-ray diffraction studies confirmed that the synthesized materials were ZnO with wurtzite phase and all the diffraction peaks agreed with the reported JCPDS data and no characteristic peaks were observed other than ZnO. The mean grain size (D) of the particles was determined from the XRD line broadening measurement using Scherrer equation[31]:

$$D=0.89\lambda / (\beta Cos\theta) \quad (1)$$

Where λ is the wavelength (Cu Kα), β is the full width at the half- maximum (FWHM) of the ZnO (101) line and θ is the diffraction angle. A definite line broadening of the diffraction peaks is an indication that the synthesized materials are in nanometer range. The lattice parameters calculated were also in agreement with the reported values. The reaction temperature greatly influences the particle morphology of as-prepared ZnO powders. Figure 2 (a &b) shows the XRD patterns of ZnO nanoparticles.

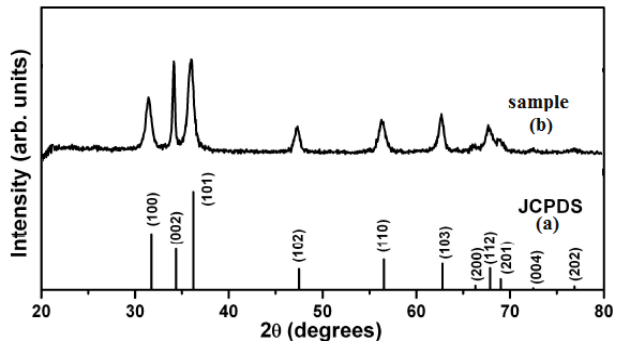

Fig. 2: XRD patterns of ZnO nanoparticles. (a) Indicate standard XRD pattern and (b) indicate sample XRD pattern.

3.3. UV–visible absorption spectra for ZnO nanoparticles:

The UV–visible absorption spectra of ZnO nanoparticles are shown in Fig. 3 although the wavelength of our spectrometer is limited by the light source, the absorption band of the ZnO nanoparticles have been shows a blue shift due to the quantum confinement of the excitons present in the sample compare with bulk ZnO particles. This optical phenomenon indicates that these nanoparticles show the quantum size effect [32].

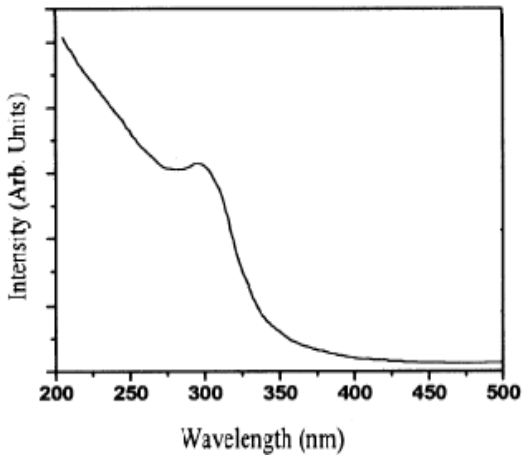

Fig. 3: UV-Vis absorption spectra for ZnO nanoparticles.

3.4. Direct electrochemistry of hemoglobin immobilized on NaY zeolite modified electrode:

Fig. 4 shows the cyclic voltammograms of different electrodes in 0.1M pH 7.0 PBS. No obvious electrochemical response was observed at both CPE and Zno Nps/ CPE (fig.4, 1). At Hb/ Zno Nps/ CPE the cyclic voltammogram showed a couple of stable redox and oxidative peaks at +240 and +342 mV at $50mVs^{-1}$(fig.4, 2). Obviously, these peaks were attributed to the redox reaction of the electroactive center of hemoglobin. Hemoglobin/ CPE also showed the response of hemoglobin, but the response was much smaller than that of Hb/ Zno Nps/ CPE (not shown). Thus, the adsorption of hemoglobin and zinc oxide nanoparticles on electrode surface played an important role in facilitating the electron exchange between the electroactive center of hemoglobin and CPE. The formal potential (E^o) of hemoglobin, estimated as the midpoint of reduction and oxidation potentials, was +(292 ± 2) mV. You can see mentioned details in figure 4.

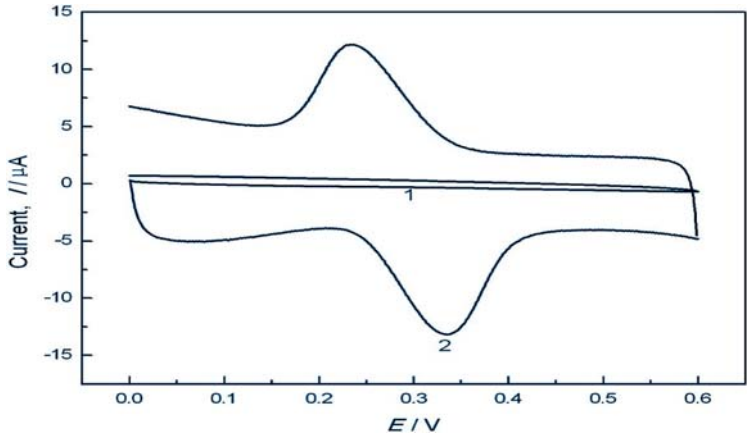

Fig. 4: Cyclic voltammograms, using (a) the Zno NPs/CPE in 0.1 M phosphate buffer and (b) Hb/ Zno Nps/ CPE in 0.1 M phosphate buffer (scan rate: 100 mV/s).

The collected voltammograms in Fig. 5 a, substantiated a statement that the nanometer-scale zinc oxide nanoparticles could play a key role in the observation of the hemoglobin CV response. On the grounds that the surface-to-volume ratio increases with the size decrease and because of the fact that the

protein size is comparable with the nanometer-scale building blocks, these nanoparticles displayed a great effect on the electron exchange assistance between hemoglobin and carbon paste electrode. For further investigate the hemoglobin characteristics at the Hb/ Zno Nps/ CPE electrode, the effect of scan rates on the hemoglobin voltammetric behavior was studied in detail. The baseline subtraction procedure for the cyclic voltammograms was obtained in accordance with the method reported by Bard and Faulkner [33]. The scan rate (ν) and the square root scan rate($\nu^{1/2}$) dependence of the heights and potentials of the peaks are plotted in Fig. 4b and c. It can be seen that the redox peak currents increased linearly with the scan rate, the correlation coefficient was 0.9979 (ipc = 0.3266ν +8.156) and 0.9979 (ipa = -0.3961ν - 6.0223), respectively. This phenomenon suggested that the redox process was an adsorption-controlled and the immobilized hemoglobin was stable. It can be seen that the redox peak currents increased more linearly with the ν in comparison to that of $\nu^{1/2}$.

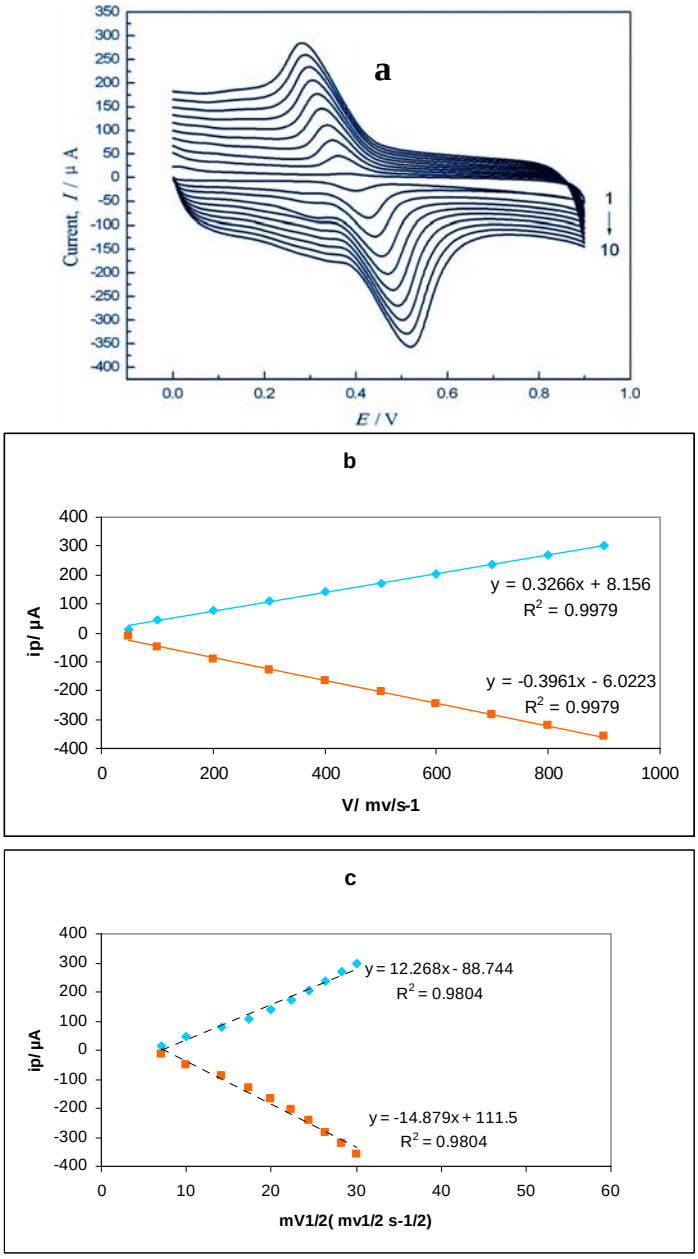

Fig. 5: (a) CVs of Hb/ Zno Nps/ CPE electrode in PBS 0.1M at various scan rates, from inner to outer; 50, 100, 200, 300,400, 500, 600, 700, 800 and 900 mV s^{-1}, the relationship between the peak currents (ipa, ipc) vs., (b) the sweep rates and (c) the square root of sweep rates. Blue lines are redox peaks and red lines are oxidative peaks.

However, there is clearly a systematic deviation from linearity in this data, i.e. low scan rates are always on one side of the line and the high scan rate points are on the other. The anodic and cathodic peak potentials are linearly dependent on the logarithm of the scan rates (ν) when ν > 1.0 V s^{-1}, which was in agreement with the Laviron theory, with slopes of -2.3RT/αnF and 2.3RT/ (1 -α) nF for the cathodic and the anodic peak, respectively [34]. So, the charge-transfer coefficient (α) was estimated as 0.5. Furthermore, the heterogeneous electron transfer rate constant (ks) was estimated according to the following equation [35-36]:

$$[\log ks = \alpha \log(1-\alpha) + (1-\alpha)\log\alpha - \log\frac{RT}{nF\nu} - \frac{\alpha(1-\alpha)nF\Delta EP}{2.3\,RT}] \quad (1)$$

Here, n is the number of transferred electrons at the rate of determining reaction and R, T and F symbols having their conventional meanings. ΔE_p is the peak potential separation. The ΔE_p was equal to -26, -94.44, -166.88, -237.33, -307.77, -378.21, -448.66, -519/05, -589.54 and -660 mV at 50, 100, 200, 300, 400, 500, 600, 700, 800 and 900 mV s^{-1}, respectively, giving an average heterogeneous transfer rate constant (ks) value of 1.56 s^{-1}.

3.5. Effect of Solution pH on Direct Electron Transfer of Immobilized Hb:

In most cases, protein redox behavior is often significantly dependent on the solution pH. Cyclic voltammograms of Hb-Zno Nps-CPE in PBS also showed a strong dependence on solution pH (Fig. 5 a,b). All changes in CV peak potentials and currents with pH were reversible in the pH range of 2 to 8.3, that is, the same CV could be obtained if the electrode was transferred from a solution with a different pH value to its original solution. An increase in solution pH caused negative shift in both cathodic and anodic peak potentials. In fig. 5 a, the calibration of response of biosensor to pH changes can be observed. In fig. 5 b, the response of biosensor to pH changes with other kind of diagram can be observed. As a result, in PH section we can say that maximum response of biosensor was at pH. 7. The electrochemical behavior in this study is also very stable against pH changes.

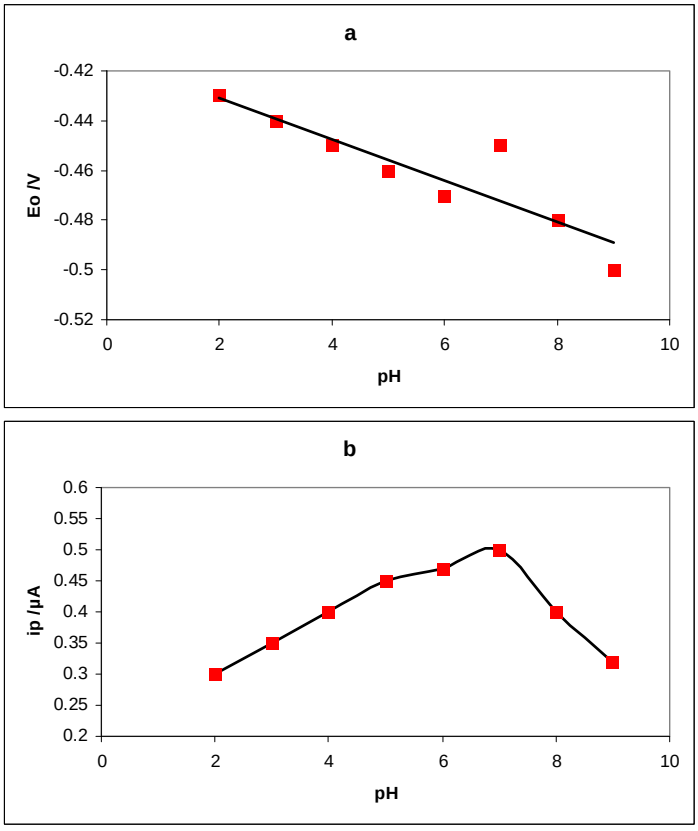

Fig. 6: (a) the calibration of response of biosensor to pH changes, and (b) show a typical diagram of response of biosensor to pH changes. The maximum of response observed at pH.7.

Adv. Environ. Biol., 6(3): 1095-1103, 2012

3.6. Electrocatalysis of Hb Immobilized in Zno nanoparticles-CPE to Reduction of H_2O_2

Reduction of H_2O_2 Upon addition of H_2O_2 to PBS, the shape of cyclic voltammogram of Hb/ Zno Nps/ CPE for the direct electron transfer of Hb changed dramatically with an increase of reduction current (Fig. 7 a), while no obvious change was observed at CPE and Zno Nps-CPE(not shown). The increase in reduction peak and the decrease in oxidation peak current of Hb at Hb/ Zno Nps/ CPE displayed an obvious electrocatalytic behavior of immobilized Hb to the reduction of H_2O_2. Furthermore, the reduction peak current increased with an increasing H_2O_2 concentration. The electrocatalytic process can be expressed as follows [6]:

$$H_2O_2+2HbHFe\ (II) \leftrightarrow 2HbFe\ (III) +2H_2O \qquad (1)$$

In the presence of H_2O_2, HbHFe(II) was efficiently converted to its oxidized form, HbFe(III). Consequently, HbFe(III) was reduced at the electrode surface by the direct electron transfer. With increasing H_2O_2 concentration the current response for HbFe(III) reduction increased (Fig. 7 a). In addition, Figure (7a) indicate that the electrocatalytic current increases with successive addition of H_2O_2. The calibration range of H_2O_2 showed in (Fig. 7 b), and it shows the sensor response. The sensor was found to have sensitivity in the range of 13 to 180 µM based upon the mean of the slope found from the points on the response curve. As can be observed, the sensor response shows good linearity in this range. The correlation factor, R^2 was found to be 0.9875.

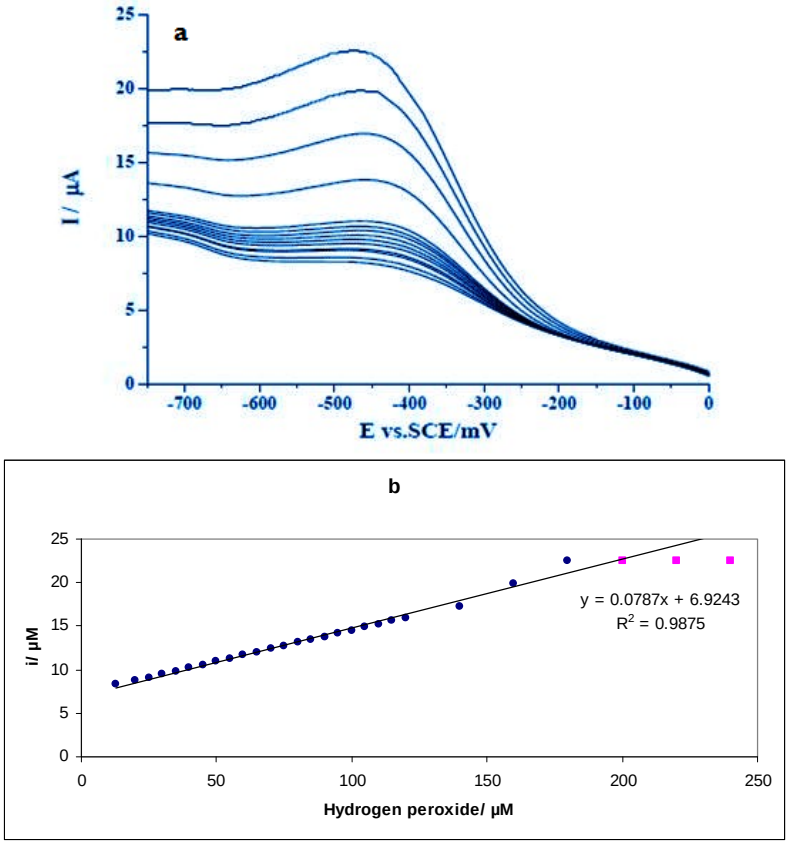

Fig. 7: (a) Cyclic voltammograms obtained at an Hb/ Zno Nps/ CPE electrode in 0.1M phosphate buffer solution (pH 7.0) for different concentrations of hydrogen peroxide and (b) the relationship between cathodic peak current of Hb and different concentrations of hydrogen peroxide (scan rate: 50 mVs^{-1}).

3.7. Effect of temperature on the H_2O_2 sensor:

Temperature is an important parameter affecting the electrocatalytic activity of enzyme or protein. Fig. 7 shows the effect of temperature on sensor response. With an increasing temperature from 10 to 45°C the response and the electrocatalytic activity of the immobilized hemoglobin increased. The immobilized hemoglobin had activity even at 45°C. It was evident that the immobilized hemoglobin had good thermal stability because of the unchanged ability of microenvironment and its native structure

upon temperature change. These results indicated that this sensor could handle in a wide range of temperature, but this novel sensor has maximum of response only at 35°C.

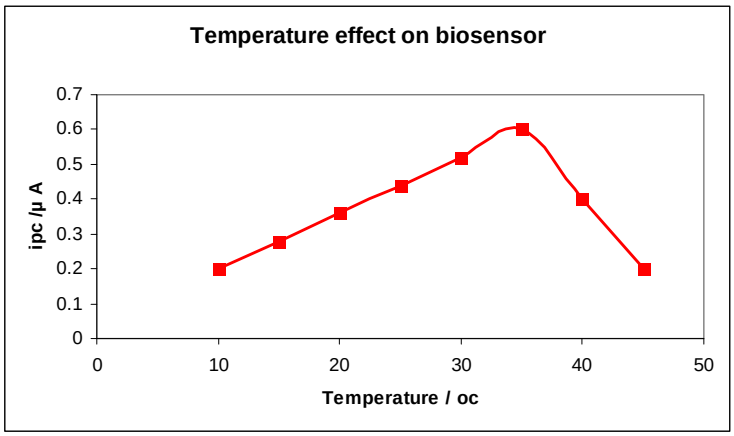

Fig. 8: Effect of temperature on biosensor at pH 7.0.

3.8. Repeatability and stability of the hydrogen peroxide biosensor:

The relative standard deviation (R.S.D.) is 2.7% for ten successive measurements at 30µM hydrogen peroxide, showing the proposed biosensor possesses a good reproducibility.

4. Conclusion:

In this work, zinc oxide nanoparticles have been synthesized and successfully used to enhance the response of a biosensor based on hemoglobin and carbon paste electrode. At Hb/Zno Nps/CPE the cyclic voltammogram exhibits a good pair of redox peaks corresponding to a surface-controlled electrode process with proton transfer. The immobilized hemoglobin displays a high affinity and sensitivity to H_2O_2. The sensor shows a good reproducibility and stability.The experiments showed excellent electrocatalytical activity of this biosensor for H_2O_2.

Acknowledgement

The Young researchers club, Marvdasht branch, Islamic Azad University, Marvdasht, Iran, supported this research work.

References

1. Giovanelli, D., N.S. Lawrence, L. Jiang, T.G.J. Jones, R.G. Compton, 2003. Amperometric determination of sulfide at a pre-oxidised nickel electrode in acidic media. Analyst, 128: 173-177.
2. Giovanelli, D., N.S. Lawrence, S.J. Wilkins, L. Jiang, T.G.J. Jones, R.G. Compton, 2003. Anodic stripping voltammetry of sulphide at a nickel film: towards the development of a reagentless sensor. Talanta, 61: 211- 220.Gopel W, Heiduschka P (1995). Interface analysis in biosensor design. Biosens. Bioelectron. 10: 853-883.
3. Yi, G.C., C. Wang and W.I. Park, 2005. "ZnO nanorods: synthesis, characterization and applications," Semiconductor Science and Technology, 20(4) S22-S34.
4. "A fluorescence-based method for determining the surface coverage and hybridization efficiency of thiol-capped oligonucleotides bound to gold thin fims and nanoparticles" L.M. Demers, C.A. Mirkin, R.C. Mucic, R.A. Reynolds, R.L. Letsinger, R. Elghanian, G. Viswanadham, Anal. Chem. 2000, 72, 5535.
5. "Selective colorimetric detection of polynucleotides based on the distancedependent optical properties of gold nanoparticles", R. Elghanian, J. J. Storhoff, R. C. Mucic, R. L. Letsinger, C. A. Mirkin, Science 1997, 277, 1078.
6. "Molecular self-assembly of aliphatic thiols on gold colloids" C. S. Weisbecker, M. V. Merritt, G. M.Whitesides, Langmuir, 1996, 12, 3763.
7. "A spectrophotometric investigation of the interaction of iodine with aromatic hydrocarbons" H. A. Benesi, J. H. Hildebrand, J. Am. Chem. Soc. 1949, 71, 2703.
8. "Anisotropic agglomeration of surface-modified gold nanoparticles in solution and on solid surfaces' K. Murakoshi, Y. Nakato, Jpn. J. Appl. Phys. 2000, 39, 4633.
9. "Color my nanoworld" A.D. McFarland, C.L. Haynes, C.A. Mirkin, R.P. Van Duyne, H.A. Godwin, J. Chem. Ed. 2004, 81, 544A.
10. Zhang, J., Y.H. Tse, W.J. Pietro and A.B.P. Lever, 1996. J. Electroanal. Chem., 406: 203.
11. Zagal, J.H. and M.A. Páez, 1997. *Electrochim. Acta*, 42: 3477.

12. Niu, L., T. You, J.Y. Gui, E. Wang and S. Dong, 1998. *J. Electroanal. Chem.,* 448: 79.
13. Lyons, M.E.G., C.A. Fitzgerald and M.R. Smyth, 1994. *Analyst,* 119: 855.
14. Wermeckers, B. and F. Beck, 1985. *Electrochim. Acta,* 30: 1491.
15. Miller, J.C., J.N. Miller and P.J. Worsfold, 1984. Statistics for Analytical Chemists, Horwood, Chichester.
16. Hachigo, A., H. Nakahata, K. Higaki, S. Fujii and S.I. Shikata, 1994. "Heteroepitaxial growth of ZnO films on diamond (111) plane by magnetron sputtering", Appl. Phys. Lett., 65: 2556.
17. Morkoc, H., S. Strite, G.B. Gao, M.E. Lin, B. Sverdlov, M. Burns, 1994. "Large-band-gap SIC, Ill-V nitride, and II-VI ZnSe-based semiconductor device technologies", J.Appl. Phys., 76: 1363.
18. Shin, W.C., M.S. Wu, 1994. *J. Cryst. Growth.,* 137: 319.
19. Huang, H.M., S. Mao, H. Feick, H. Yan, Y. Wu, H. Kind, E. Weber, R. Russo, P.D. Yang, 2001. *Science* 292: 1897.
20. Hung, N.T., N.D. Quang, S. Bernik, 2001. *J. Mater. Res.,* 16: 2817.
21. Cooray, N.F., K. Kushiya, A. Fujimaki, D. Okumura, M. Sato, M. Ooshita, O. Yamase, 1999. *Jpn. J. Appl. Phys.,* 38: 6213.
22. Paneva, R., D. Gotchev, 1999. *Sens. Actuat. A: Phys.,* 72: 79.
23. Topoglidis, E., A.E.G. Cass, B. Oregan, J.R. Durrant, 2001. *J. Electroanal. Chem.,* 517: 20.
24. Gao, L., Q. Li, W.L. Luan, 2002. *J. Am. Ceram. Soc.,* 85: 1016. 17. C.X. Xu, X.W. Sun, *Appl. Phys. Lett.,* 83: 3806.
25. Gao, P.X., Y. Ding, W. Mai, W.L. Hughes, C.S. Lao, Z.L. Wang, 2005. *Science,* 309: 1700.
26. Hill, H.A.O., 1996. *Coord. Chem. Rev*., 151: 115.
27. Song, S., R.A. Clark, E.F. Bowden, M.J. Tarlov, 1993. *J. Phys.Chem*., 97: 6564.
28. Yu, J., H. Ju, 2002. *Anal. Chem*., 74: 3579.
29. Masoud Negahdary, Somaye Rad, Mahdi Torkamani Noughabi, Ali Sarzaeem, Saeid Pasban Noughabi, Fazlollah Mirzaeinasab, Manouchehr Mazdapour and Somaye Amraeifard, 2012. Design a Hydrogen Peroxide Biosensor by Cytochrome c and Cadmium Oxide Nanoparticles and its Application in Diagnostic Cancer Cells. Advanced Studies in Biology, 4(3): 103-118.
30. Nanjundiah, C., S.F. McDevitt, V.R. Koch, 1997. J. Electrochem. Soc., 144: 3392.
31. Mikoshiba, S., S. Murai, H. Sumino, S. Hayase, 2002. Chem. Lett., 31: 1156.
32. Haiming Fan, Lintao Yang, Nanotechnology, 15: 37.
33. Meulenkamp, E.A., 1998. J. Phys. Chem., 102: 7764.
34. Bard, A.J., L.R. Faulkner, 2001. Electrochemical Methods, second. ed., Fundamentals and Applications, Wiley, NY, pp: 241.
35. Laviron, E., 1979. J. Electroanal. Chem., 101: 19-28.
36. Laviron, E., 1979. J. Electroanal. Chem., 100: 263-270.